

Expanding the genetic landscape of endometriosis: Integrative -omics analyses uncover key pathways from a multi-ancestry study of over 900,000 women

Authors and Affiliations

Lindsay A Guare¹, Jagyashila Das¹, Lannawill Caruth¹, Ananya Rajagopalan², Alexis T. Akerele³, Ben M Brumpton⁴, Tzu-Ting Chen⁵, Leah Kottyan⁶, Yen-Feng Lin⁵, Elisa Moreno⁴, Ashley J Mulford⁷, Vita Rovite⁸, Alan R Sanders⁷, Marija Simona Dombrovska⁸, Noemie Elhadad⁹, Andrew Hill¹⁰, Gail Jarvik¹¹, James Jaworski¹², Yuan Luo¹³, Shinichi Namba¹⁴, Yukinori Okada¹⁴, Yue Shi¹⁵, Yuya Shirai¹⁶, Jonathan Shortt¹⁰, Wei-Qi Wei¹⁷, Chunhua Weng⁹, Yuji Yamamoto¹⁶, Sinead Chapman¹⁵, Wei Zhou¹⁵, Digna R. Velez Edwards¹⁸, Shefali Setia-Verma¹

Corresponding Author: Shefali Setia-Verma

¹Pathology and Laboratory Medicine, University of Pennsylvania, Philadelphia, PA, United States, ²Genomics and Computational Biology, University of Pennsylvania, Philadelphia, PA, United States, ³Division of Quantitative Science, Department of Obstetrics and Gynecology, Department of Microbiology, Immunology, and Physiology, Vanderbilt University Medical Center, and Meharry Medical College, Nashville, TN, United States, ⁴HUNT Center for Molecular and Clinical Epidemiology, Norwegian University of Science and Technology, Trondheim, Norway, ⁵Center for Neuropsychiatric Research, National Health Research Institutes, Maoli County, Taiwan, ⁶Cincinnati Children's Hospital Medical Center, Cincinnati, OH, United States,

22 ⁷Endeavor Health, Evanston, IL, United States, ⁸Latvian Biomedical Research and Study Centre,
23 Riga, Riga, Latvia, ⁹Biomedical Informatics, Columbia University, New York City, NY, United
24 States, ¹⁰Colorado for Precision Medicine, Aurora, CO, United States, ¹¹Division of Medical
25 Genetics, University of Washington, Seattle, WA, United States, ¹²Division of Epidemiology,
26 Department of Medicine, Vanderbilt University Medical Center, Nashville, Tennessee, United
27 States, ¹³Feinberg School of Medicine, Northwestern University, Evanston, IL, United States,
28 ¹⁴Genome Informatics, The University of Tokyo, Tokyo, Japan, ¹⁵Broad Institute, Cambridge,
29 MA, United States, ¹⁶Statistical Genetics, Osaka University, Suita, Osaka, Japan, ¹⁷Biomedical
30 Informatics, Vanderbilt University, Nashville, TN, United States, ¹⁸Division of Quantitative
31 Science, Department of Obstetrics and Gynecology, Vanderbilt University Medical Center,
32 Nashville, Tennessee, United States

33 **Abstract**

34 We report the findings of a genome-wide association study (GWAS) meta-analysis of
35 endometriosis consisting of a large portion (31%) of non-European samples across 14 biobanks
36 worldwide as part of the Global Biobank Meta-Analysis Initiative (GBMI). We identified 45
37 significant loci using a wide phenotype definition, seven of which are previously unreported and
38 detected first genome-wide significant locus (*POLR2M*) among only African-ancestry. Our
39 narrow phenotypes and surgically confirmed case definitions for endometriosis analyses
40 replicated the known loci near *CDC42*, *SKAP1*, and *GREB1*. Through this large ancestry stratified
41 analyses, we document heritability estimates in range of 10-12% for all ancestral groups. Thirty-
42 eight loci had at least one variant in the credible set after fine-mapping. An imputed

43 transcriptome-wide association study (TWAS) identified 11 associated genes (two previously
44 unreported), while the proteome-wide association study (PWAS) suggests significant
45 association of R-spondin 3 (RSPO3) with wide endometriosis, which plays a crucial role in
46 modulating the Wnt signaling pathway. Our diverse, comprehensive GWAS, coupled with
47 integrative -omics analysis, identifies critical roles of immunopathogenesis, Wnt signaling, and
48 balance between proliferation, differentiation, and migration of endometrial cells as hallmarks
49 for endometriosis. These interconnected pathways and risk factors underscore a complex,
50 multi-faceted etiology of endometriosis, suggesting multiple targets for precise and effective
51 therapeutic interventions.

52 **Introduction**

53 Endometriosis, a debilitating condition characterized by the growth of endometrial-like tissues
54 outside of the uterus affects approximately 10% of women of reproductive age worldwide^{1,2}.
55 The precise mechanisms of these lesions are presently unknown. Endometriosis is incurable,
56 leaving patients to manage severe pain³ and cope with fertility challenges⁴. Despite its
57 prevalence and impact, the etiology of endometriosis remains poorly understood, hampering
58 efforts to develop effective diagnostic tools and targeted treatments.

59 Genome-wide association studies (GWASs) have been an important tool for implicating
60 candidate genes and pathways linked with endometriosis. GWASs for endometriosis have
61 uncovered over 40 loci associated with endometriosis risk. However, like most GWASs
62 historically, the previous endometriosis studies have primarily included European populations
63 with some East-Asian datasets as well⁵. Consequently, they have explained about 7% of

64 phenotypic variance with common variants^{6,7} and have fallen short in elucidating the full
65 spectrum of its pathophysiology.

66 The advent of large-scale biobanks has revolutionized genetic research, offering unique
67 opportunities to conduct well-powered studies across diverse populations. As more diverse
68 genomic datasets are developed, like the Penn Medicine Biobank (PMBB)⁸, the All of Us
69 Research Program (AOU)⁹, and the Million Veterans Program (MVP)¹⁰, that diversity can
70 increase statistical power and enhance the discovery of trait loci¹¹. A worldwide consortium of
71 genomic researchers, the global biobank meta-analysis initiative (GBMI), was established to
72 facilitate collaboration in GWAS studies on unprecedented scales. In this study, we have
73 collaborated with 12 biobanks across several countries^{9,12-22}. These resources not only enhance
74 statistical power to detect novel associations but also provide rich phenotypic data, enabling
75 more refined analyses. Moreover, the inclusion of diverse ancestries in genetic studies is crucial
76 for improving the generalizability of findings and addressing health disparities. This is
77 particularly pertinent for endometriosis, where significant variations in prevalence and clinical
78 presentation have been observed across different ethnic groups²³.

79 Beyond GWAS, there are many methods which can be employed *in silico* to investigate
80 other elements of the central dogma, providing further validation of GWAS loci and discovery of
81 additional disease-associated genes. Recent advances in multi-omics technologies have further
82 expanded our ability to translate genetic associations into biological insights. Integration of
83 GWAS results with transcriptomic, proteomic, and single-cell data using methods such as allows
84 for a more comprehensive understanding of disease mechanisms, potentially identifying novel
85 therapeutic targets and biomarkers. Then, these multi-omic layers of association can be

86 integrated using tools such as Mergeomics²⁴, which also identifies gene sets enriched for
87 association with the disease of interest. For endometriosis, where the interplay between
88 genetic predisposition and complex tissue-specific processes is central to its pathogenesis, such
89 integrative approaches are especially valuable. Given these considerations, there is a critical
90 need for a large-scale, ancestrally diverse GWAS of endometriosis that incorporates rigorous
91 phenotyping and leverages multi-omics data to provide a more complete picture of the
92 disease's genetic landscape and underlying biology.

93 Here, we present the results of large-scale GWAS meta-analyses that significantly
94 advances our understanding of endometriosis pathophysiology. Our study encompasses a
95 diverse cohort from 14 biobanks worldwide, with over 30% non-European participants,
96 enhancing the generalizability of our findings. We employed a comprehensive phenotyping
97 approach, including not only a wide spectrum of endometriosis presentations but also surgically
98 confirmed and procedure-validated (surgery or imaging) phenotypes. This rigorous phenotyping
99 strategy allows for a more nuanced exploration of the genetic architecture underlying various
100 manifestations of endometriosis. Through integrative multi-omics analyses, incorporating
101 transcriptomic, proteomic, and single-cell data from endometrial tissues, we have explored five
102 major hallmarks of endometriosis pathogenesis. These findings provide unprecedented insights
103 into the molecular mechanisms driving this complex disorder, paving the way for improved
104 diagnostics and targeted therapeutic interventions.

105 Results

106 EHR-Based Phenotyping of Endometriosis in Genetically Diverse Datasets

107 We considered six phenotype definitions for our GWASs: wide endometriosis (W), wide
108 endometriosis excluding cases and controls with adenomyosis (Wex), procedure-confirmed
109 narrow endometriosis versus all controls (PCN.v1) and versus procedure-confirmed controls
110 (PCN.v2), and surgically-confirmed narrow endometriosis versus all controls (SCN.v1) and
111 versus surgically-confirmed controls (SCN.v2). The largest phenotype, W, comprised 928,413
112 women, including 44,125 cases. We leveraged publicly-available FinnGen²⁵ and MVP¹⁰ summary
113 statistics to increase the sample size. The Wex phenotype, for which several biobanks were
114 omitted, had a total sample size of 434,444 ($N_{\text{cases}} = 8,122$). Sample sizes for the PCN and SCN
115 phenotypes were smaller (Table 1), with summary statistics included from only eight of the 12
116 contributing GBMI biobanks (Supplementary Table 1).

117 Table 1: All GWAS meta-analysis sample sizes. All six phenotypes had a multi-ancestry meta-analysis as well as
118 single-ancestry meta-analyses for AFR, AMR, EAS, and EUR. There were not enough EAS studies to conduct meta-
119 analyses for the surgically confirmed narrow (SCN) phenotypes.

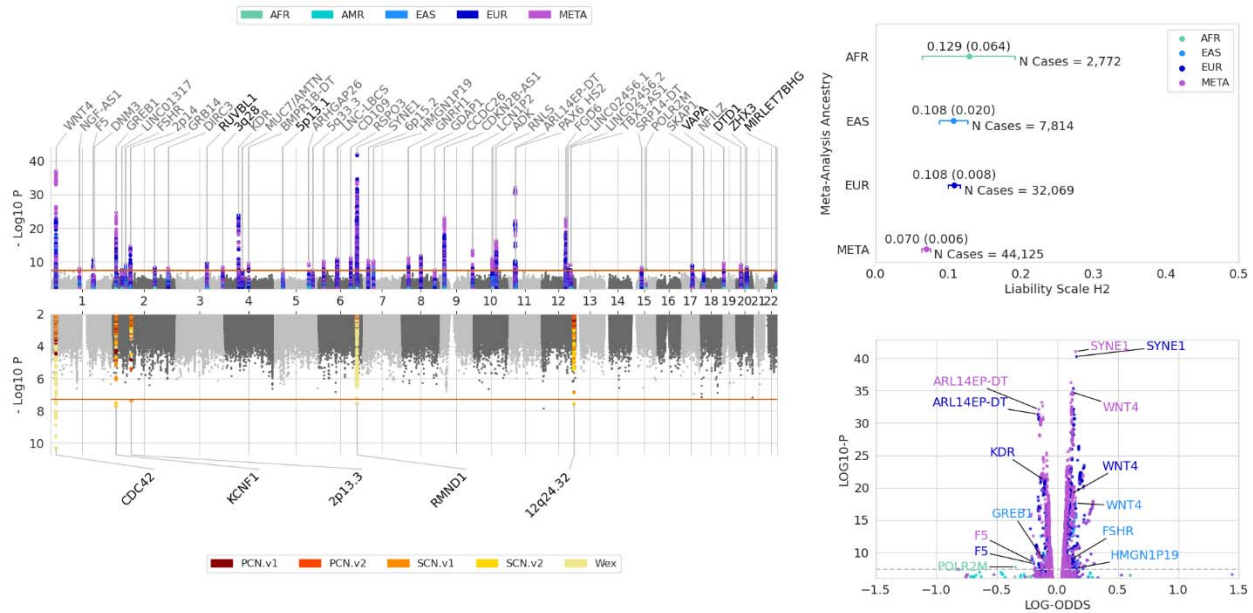
Phenotype	Ancestry	N	Cases	Prevalence
W	AFR	74,976	2,772	3.70%
	AMR	38,837	1,262	3.25%
	CSA	5,222	208	3.98%
	EAS	165,464	7,814	4.72%
	EUR	643,914	32,069	4.98%
	META	928,413	44,125	4.75%
Wex	AFR	56,314	862	1.53%
	AMR	38,195	620	1.62%
	CSA	5,066	62	1.22%
	EAS	80,375	1,531	1.90%
	EUR	254,494	5,047	1.98%
	META	434,444	8,122	1.87%
PCN.v1	AFR	51,050	823	1.61%
	AMR	36,719	599	1.63%
	EAS	78,999	155	0.20%

	EUR	209,207	3,207	1.53%
	META	375,975	4,784	1.27%
PCN.v2	AFR	9,874	823	8.34%
	AMR	7,113	599	8.42%
	EAS	1,539	155	10.07%
	EUR	35,722	3,207	8.98%
	META	54,248	4,784	8.82%
SCN.v1	AFR	50,592	365	0.72%
	AMR	36,465	345	0.95%
	EUR	208,136	2,137	1.03%
	META	295,193	2,847	0.96%
SCN.v2	AFR	1,436	365	25.42%
	AMR	1,957	345	17.63%
	EUR	12,926	2,137	16.53%
	META	16,319	2,847	17.45%

120 Multi-Ancestry GWAS Meta-Analysis Results

121 All 4,983 genome-wide significant variants ($P < 5 \times 10^{-8}$) from all meta-analyses are listed in
122 Supplementary Table 2. The primary meta-analysis performed (multi-ancestry, wide phenotype)
123 yielded 96 regions. From there, physically overlapping clumps were merged, resulting in 42 loci
124 significantly associated with endometriosis. Besides those 42, there were two EUR-specific loci
125 (*LINC01317* and *LINC02456*) and one AFR-specific locus (*POLR2M*), totaling 45 loci annotated in
126 Figure 1a (Supplementary Table 3). All EAS loci overlapped with loci from the multi-ancestry
127 meta-analyses, and the AMR W GWAS did not yield any genome-wide significant loci. Of the 45
128 unique W loci, 24 of their lead SNPs were in LD ($R^2 > 0.25$) with the lead SNPs reported in
129 *Rahmioglu et al, 2023*, and an additional 14 were found within 50 Mb of the 2023 GWAS lead
130 SNPs. The seven remaining loci were unreported in the 2023 GWAS: *RUVBL1* (rs4058156, $P =$
131 $3.51E-10$), *3q28* (rs9870207, $P = 4.17E-09$), *5p13.1* (rs55920409, $P = 2.66E-08$), *VAPA*
132 (rs79380316, $P = 3.56E-08$), *DTD1* (rs6112068, $P = 8.72E-10$), *ZHX3* (rs17265513, $P = 5.58E-09$),
133 *MIRLET7BHG* (rs873492, $P = 4.80E-08$). The observed SNP heritability, computed with LDSC, was
134 significantly greater than zero ($P < 0.05$) in the multi-ancestry meta-analysis ($h^2_{lia} = 0.070$) as
135 well as the AFR ($h^2_{lia} = 0.129$), EAS ($h^2_{lia} = 0.108$), and EUR ($h^2_{lia} = 0.108$) single-ancestry meta-
136 analyses (Figure1b).

137



138
 139 Figure 1: main meta-analysis results. Top left: overlaid Manhattan plots for the five W GWASs (multi-ancestry +
 140 four single-ancestries). Significant loci are highlighted, with black text representing the previously unreported hits.
 141 Bottom left: Overlaid Manhattan plots for the five multi-ancestry GWASs for the other phenotypes. All loci are
 142 previously reported. Top right: LDSC heritability estimates for the W GWASs; AMR is excluded because the
 143 heritability estimate was not significant. Bottom right: volcano plot highlighting variants with an absolute log-odds
 144 effect size > 0.1, colored by ancestry group.

145 Precise Phenotype Analyses Replicate Known Loci

146 For the other phenotype meta-analyses, we identified seven significant loci: two for EUR and
 147 multi-ancestry (SCN.v2 and SCN.v1), one for AFR and multi-ancestry (SCN.v1), three just in
 148 multi-ancestry (two Wex and one SCN.v1), and one just in AMR (PCN.v1). Both loci associated
 149 with Wex in the multi-ancestry analysis replicate known signals. *CDC42* (rs56319427, $P = 4.91E-$
 150 11) is in LD ($R^2 = 0.91$) with the previous *CDC42* locus, and *RMND1* (rs9322319, $P = 2.86E-08$) is
 151 near the previous *SYNE1* locus. The five loci identified with the narrow phenotypes are within
 152 50Mb of known signals, so they are not considered previously unreported. The surgically-
 153 confirmed cases vs all controls phenotype (SCN.v1) yielded two loci: 2p13.3 (rs116763937, $P =$
 154 4.07E-08), also significant in AFR, and *CD163* (rs118078722, $P = 1.39E-08$), also significant in
 155 EUR. When comparing surgically-confirmed cases with only surgically-confirmed controls

156 (SCN.v2), we identified two loci: *KCNF1* (rs115117372, $P = 1.97E-08$) and 12q24.32 (rs12581759,
 157 $P = 2.64E-08$), with *KCNF1* also significant in the *EUR* meta-analysis. The final locus, *OTUD7A*
 158 (rs17762839, $P = 1.72E-08$), was associated with the PCN.v1 phenotype in the AMR meta-
 159 analysis. These loci are displayed in Figure 1c.

160 Fine-Mapping to Detect Causal Variants at GWAS Loci

161 To elucidate shared and population-specific putative causal variants, we conducted statistical
 162 fine-mapping on all hits from multi-population meta-analyses, totaling 48 loci in five (PCN.v2
 163 had no significant hits) studies (See Methods). Of those 48 loci, 38 had at least one variant with
 164 posterior probability of being causal (PIP) greater than 0.5, totaling 132 causal variants
 165 (Supplementary Table 4). The cross-ancestry fine-mapping analyses computed PIPs for each
 166 variant across all combinations of ancestry groups included in the overall study. We identified
 167 credible sets (CS) for the 38 distinct loci associated with endometriosis as reported in Table 2.

168 Table 2: credible sets of multi-ancestry GWAS loci. 34 are for the W phenotype, 2 are for Wex, and 2 are for SCN.v2
 169 (SCN cases versus surgically-confirmed controls). An “X” in the AFR-EUR columns denote whether that ancestry
 170 group was used for detecting any SNPs in the credible set ($PIP > 0.5$). Locus names match the GWAS.

Phenotype	Locus	Locus P	# CS	AFR	AMR	EAS	EUR	Credible Set
W	<i>WNT4</i>	1.12E-37	3			X	X	rs2473331, rs61768001, rs16826658
W	<i>MIR4418</i>	1.85E-09	3	X		X	X	rs1934478, rs10917216, rs12097230
W	<i>NGF-AS1</i>	1.11E-08	4			X	X	rs12030576, rs11102915, rs6656381, rs12075799
W	<i>DNM3</i>	2.38E-08	2		X	X	X	rs479960, rs569179
W	<i>GREB1</i>	2.45E-25	2		X	X	X	rs10929759, rs10165819
W	<i>FSHR</i>	8.59E-10	6	X	X	X	X	rs12614817, rs6716567, rs2134811, rs13032266, rs4420736, rs6722885
W	<i>2p14</i>	2.23E-15	2			X	X	rs2683680, rs2860517
W	<i>DIRC3</i>	6.11E-09	3			X	X	rs13018792, rs67436597, rs72613753
W	<i>EEFSEC</i>	1.00E-09	2		X		X	rs2955102, rs2811529
W	<i>3q28</i>	4.17E-09	7			X	X	rs9870207, rs6778588, rs9290954, rs9837216, rs9872656, rs9834978, rs9830307

W	<i>KDR</i>	6.46E-24	2	X	X	X	X	rs7680198, rs17081840
W	<i>MUC7/AMT N</i>	4.27E-08	4	X			X	rs13105826, rs4694318, rs28751942, rs28503247
W	<i>BMPR1B-DT</i>	3.88E-10	3			X	X	rs11938840, rs6532503, rs7680214
W	<i>5p13.1</i>	2.66E-08	2			X	X	rs13165498, rs2220801
W	<i>ARHGAP26</i>	5.06E-10	2			X	X	rs7728894, rs1799293
W	<i>5q33.3</i>	3.49E-08	6	X		X	X	rs1316379, rs13170063, rs2963462, rs2901003, rs11135035, rs17055653
W	<i>SYNE1</i>	9.67E-43	7		X	X	X	rs9371219, rs7740302, rs9371528, rs6927162, rs58415480, rs9371246, rs6557210
W	<i>6p15.2</i>	4.40E-11	5			X	X	rs1812673, rs13231733, rs11976790, rs1451383, rs1451385
W	<i>HMGN1P19</i>	5.37E-11	2			X	X	rs10951860, rs11975261
W	<i>GNRH1</i>	6.06E-12	2			X	X	rs7819740, rs13277090
W	<i>CDKN2B-AS1</i>	9.16E-24	9			X	X	rs7028213, rs10122243, rs10757288, rs1333054, rs1537377, rs10965274, rs2779747, rs10738612, rs1095899
W	<i>LCN1P2</i>	4.67E-14	1			X	X	rs633862
W	<i>RNLS</i>	5.69E-17	6			X	X	rs792208, rs792212, rs111958828, rs10788601, rs7922551, rs1935578
W	<i>ARL14EP-DT</i>	8.96E-33	5	X		X	X	rs606651, rs606642, rs476669, rs601681, rs76242056
W	<i>PAX6_HS2</i>	1.86E-09	2			X	X	rs6484567, rs2207550
W	<i>FGD6</i>	1.41E-23	2	X		X	X	rs10777675, rs6538622
W	<i>LINC02456</i>	7.72E-10	5	X		X	X	rs7306496, rs12319554, rs10437892, rs7296495, rs11111353
W	<i>TBX3-AS1</i>	9.23E-10	3			X	X	rs11067288, rs11067298, rs117549885
W	<i>SRP14-DT</i>	4.16E-09	5	X	X	X	X	rs4924409, rs2412474, rs78053299, rs12441483, rs7162269
W	<i>VAPA</i>	3.56E-08	2			X	X	rs604079, rs486270
W	<i>NFILZ</i>	2.25E-10	1			X	X	rs2967676
W	<i>DTD1</i>	8.72E-10	4			X	X	rs6075379, rs6081270, rs34478401, rs6045578
W	<i>ZHX3</i>	1.29E-08	3			X	X	rs6102464, rs6102467, rs4610114
W	<i>MIRLET7BHG</i>	4.80E-08	3	X	X		X	rs11702897, rs9626905, rs3859891
Wex	<i>CDC42</i>	4.91E-11	2			X	X	rs3754496, rs7529389
Wex	<i>RMND1</i>	2.86E-08	3	X	X	X	X	rs3778608, rs6913515, rs6904364
SCNv2	<i>KCNF1</i>	1.97E-08	5		X		X	rs13387419, rs77606953, rs10194777, rs2091817, rs1317430
SCNv2	<i>12q24.32</i>	2.64E-08	2		X			rs10773384, rs10847311

171 Of the 38 loci with at least one variant in the credible set, 34 were from the W multi-
172 population meta-analysis, 2 were from Wex, and 2 were from SCN.v2. Fourteen of the credible

173 sets included variants detectable in part due to new genetic ancestry groups incorporated in
174 the analyses (AMR and AFR). In particular, three loci leveraged the incorporation of all four
175 ancestries to compute the credible set: *FSHR*, *KDR*, and *SRP14-DT*.

176 GWAS Variant Gene Enrichment Analyses

177 From the wide multi-population meta-analysis, we identified 47 unique gene regions
178 that were enriched for significant GWAS variants. Eight genes were specific to the multi-
179 ancestry W meta-analysis: *CDKN2A*, *CCHCR1*, *AP3M1*, *SPECC1*, *IGF1*, *DTD1*, *DNM3*, and *TCF19*.
180 Eleven were specific to the EUR meta-analysis: *CBX1*, *GRB14*, *HOXA5*, *RPS10*, *SNX11*, *CHD6*, *VIP*,
181 *LOC105375205*, *PARPBP*, *NOL4L*, *NR2C1*, and one (*CEBPE*) was specific to the AMR meta-
182 analysis. Two additional genes were identified for the other phenotypes: *TCEA2* with Wex in the
183 multi-ancestry meta-analysis, and *HAVCR2* in the PCN.v1 EAS meta-analysis. Full MAGMA
184 results are given in Supplementary Table 5.

185 Post-GWAS Multi-Omic Analyses Fuel Pathway Identification

186 To identify associations between endometriosis and both the transcriptome and proteome, we
187 performed TWAS using uterine tissue eQTL weights from GTEx and PWAS on whole blood
188 pQTLs, inputting the multi-ancestry W GWAS summary statistics (See Methods). The TWAS
189 tested 9,642 genes, and the PWAS tested 300 proteins. There were 11 genes achieving genome-
190 wide significance (Bonferroni P value < 0.05) in the TWAS and 1 in the PWAS, shown in Table 3.

191 Table 3: 11 significant TWAS genes and one significant PWAS protein. The p-value thresholds were adjusted for the
192 numbers of tests (TWAS P < 0.05 / 9,642, and PWAS P < 0.05 / 300).

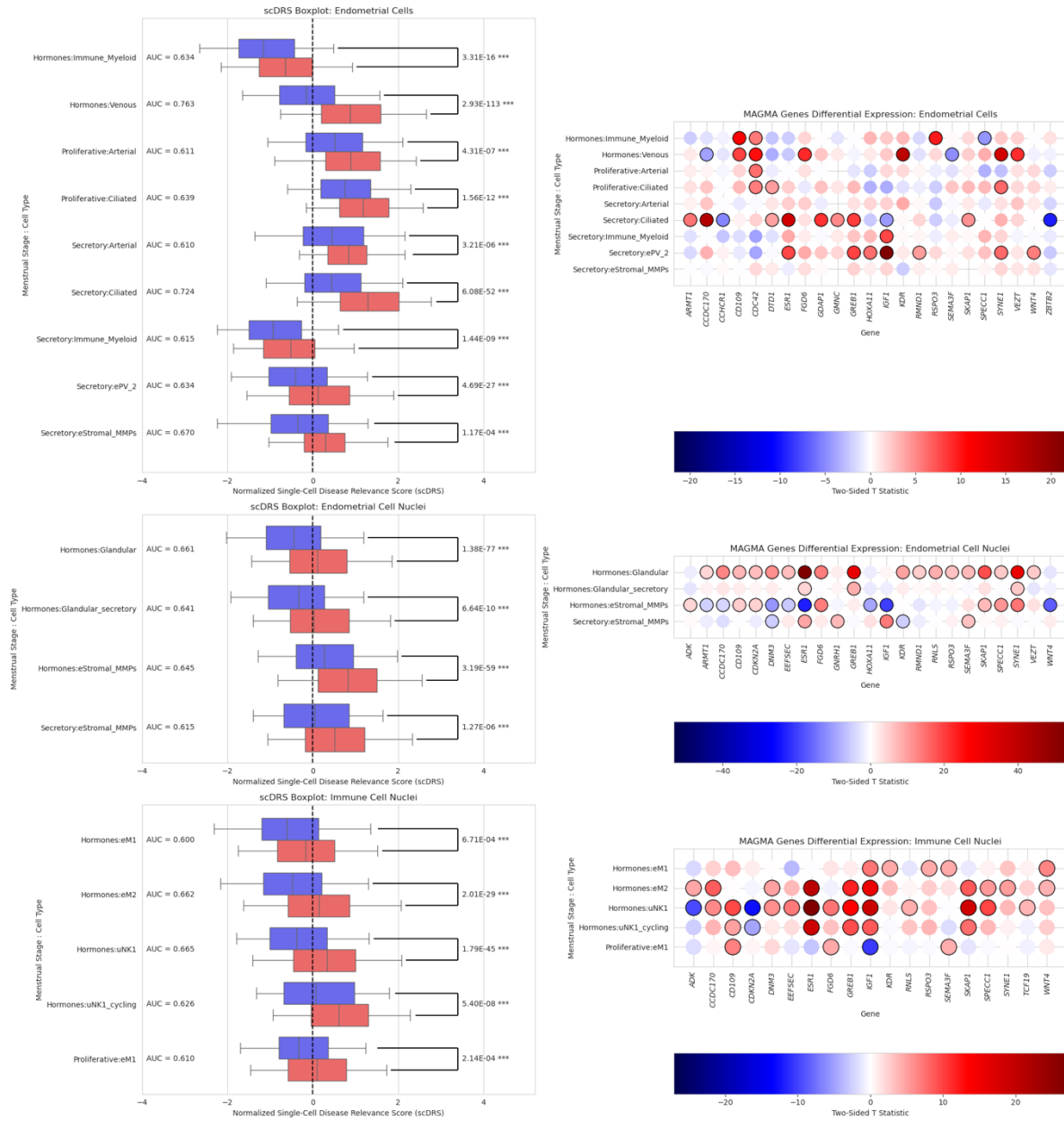
Gene Symbol	Z-score	Beta	P-value
<i>RMND1</i>	8.69	4.92	3.7E-18
<i>ARL14EP</i>	-8.35	0.16	6.8E-17

<i>ZBTB2</i>	-6.86	1.77	6.7E-12
<i>VEZT</i>	6.62	0.44	3.5E-11
<i>KDR</i>	-6.17	0.54	6.7E-10
<i>ARMT1</i>	6.13	0.77	8.9E-10
<i>RP11-521C20.2</i>	-5.11	0.27	3.3E-07
<i>RP11-521C20.5</i>	-5.11	0.13	3.3E-07
<i>CCDC88B</i>	-4.79	0.20	1.7E-06
<i>DTD1</i>	4.77	0.20	1.9E-06
<i>NOL4L</i>	4.57	0.77	4.8E-06
<i>RSPO3</i>	6.08	0.14	1.2E-09

193 Of 11 significant genes identified from TWAS, nine of them were proximal to our
194 significant multi-ancestry W GWAS loci. Three of them are the nearest genes to GWAS loci:
195 *ARL14EP*, *KDR*, and *DTD1*. Three TWAS genes (*RMND1*, *ZBTB2*, and *ARMT1*) are related to the
196 chromosome six cluster of loci which also includes *SYNE1* and *ESR1*. In the GWAS results, *RMD1*
197 was more prominent in the Wex phenotype. *VEZT* (TWAS P = 3.5E-11) was most significant in
198 the EAS GWAS results and was overlapping with the multi-ancestry GWAS locus *FGD6*. Two
199 lincRNA genes identified in TWAS, *RP11-521C20.2*, *RP11-521C20.5*, are close to the GWAS locus
200 *SRP14-DT*. The remaining two TWAS genes, *NOL4L* and *CCDC88B*, are not proximal to any GWAS
201 loci we identified (at least 20 Mb away). PWAS identified *RSPO3* (P = 1.2E-09) as the only
202 significantly-associated protein, which was also a significant locus from our GWAS meta-
203 analysis.

204 Identifying Disease-Relevant Cell Types and Crucial Genes

205 We prioritized 18 cell type – menstrual stage pairs with AUROC > 0.6 in which to compare gene
206 expression for the 35 top MAGMA genes in the multi-ancestry W meta-analysis.



207

208

209

210

211

212

213

214

215

216

Figure 3: single cell analyses – disease relevance scores (scDRSs) and differential gene expression. The left panels show the distributions of scDRS comparing cells from donors with endometriosis (red) to donors without endometriosis (blue). Each set of boxes is annotated on the y-axis with the menstrual stage and cell type, an AUROC for the scDRS, and a P-value for a one-sided t-test of independent means. The right panels show the results of two-sided t-tests comparing the gene expression of the top MAGMA genes, with significant tests circled with a black border.

Of the 18 cell type – menstrual stage pairs with significantly different mean scDRS and AUROC > 0.6, nine came from donors in the “Hormones” menstrual phase (two endometrial cell types, three endometrial nucleus types, and four immune nucleus types). Of those nine, the

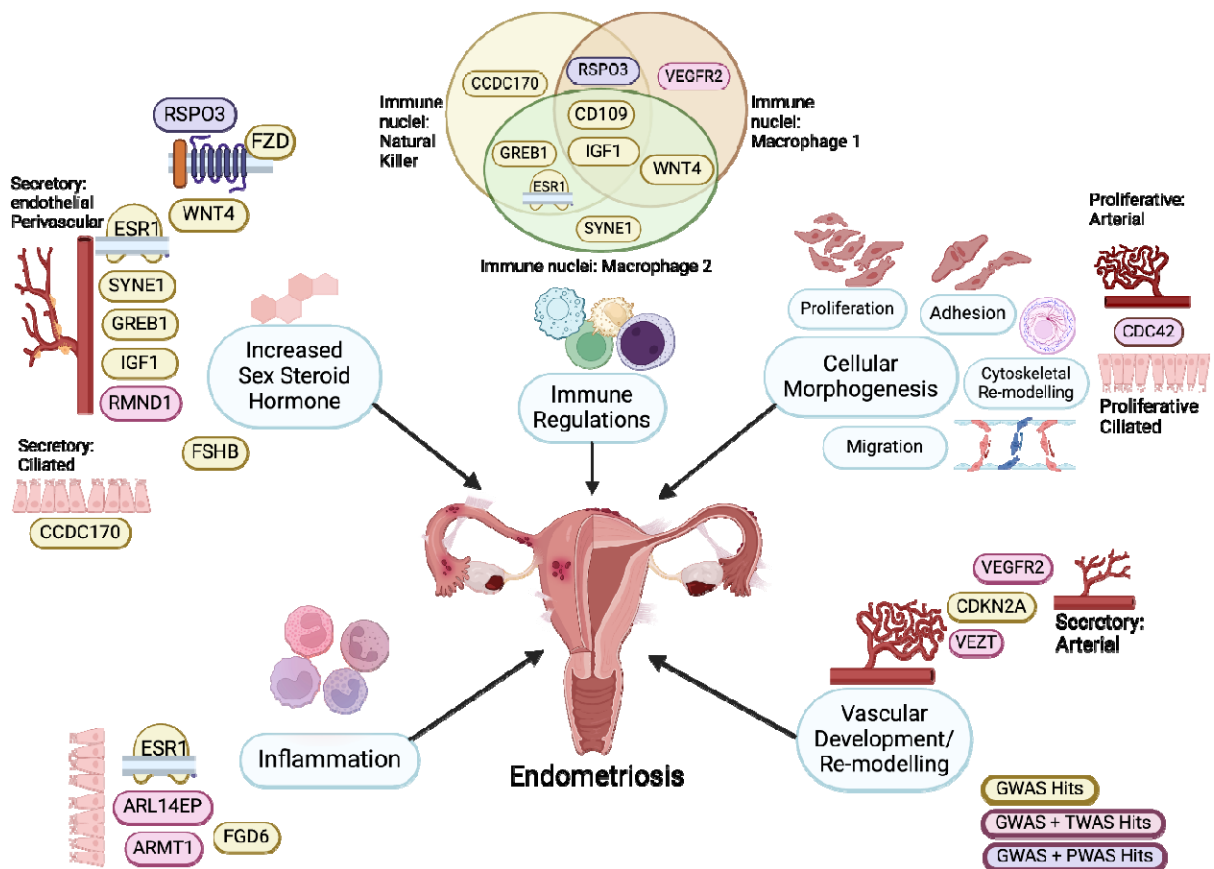
217 gene *CD109* was more highly expressed in six: immune myeloid cells, venous cells, glandular
218 nuclei, stromal MMP (matrix metalloproteinase – expressing) nuclei, uterine natural killer
219 nuclei, and cycling uterine natural killer nuclei.

220 The expression of *IGF1* was significantly different between cells from endometriosis
221 cases and controls in ten cell type – menstrual stage pairs (three endometrial cell types, two
222 endometrial nucleus types, and all five immune nucleus types). It did not always have the same
223 direction; for seven out of those ten groups, expression of *IGF1* was greater, while for the
224 remaining three (secretory phase ciliated cells, stromal MMP nuclei from donors on hormones,
225 and proliferative phase uterine macrophage nuclei), it was downregulated.

226 *WNT4* and *ESR1* are well-known endometriosis-associated genes. *WNT4*'s expression
227 was significantly different between endometriosis cases and controls in four cell type –
228 menstrual stage pairs. *WNT4* expression was higher in both macrophage nucleus populations
229 (eM1 and eM2) in donors taking exogenous hormones and secretory phase perivascular
230 (ePV_2) nuclei. In contrast, *WNT4* expression was lower in stromal MMP nuclei from donors on
231 hormones. *ESR1* expression was significantly different in nine cell type – menstrual stage pairs
232 (three secretory, six hormones). All but one association were positive – the one negative T
233 statistic was found in stromal MMP nuclei from donors on hormones. The three secretory
234 groups with *ESR1* upregulated in donors with endometriosis were ciliated cells, perivascular
235 (ePV_2) cells, and stromal MMP nuclei.

236 **Mergeomics identifies significant biological processes from multi-omic**
237 **integration**

238 Using marker set enrichment analysis (MSEA) on KEGG database gene sets²⁶, we identified one
239 significantly enriched pathway that provides insight into the molecular mechanisms underlying
240 endometriosis. The WNT signaling pathway (hsa04310) was the most significantly enriched
241 biological process, driven by markers including *RUVBL1*, *WNT4*, and *CTBP2* (Supplementary
242 Figure XX). Other significant pathways (FDR $P < 0.05$) were Focal Adhesion (hsa04510), B cell
243 receptor signaling pathway (hsa04662), Notch signaling pathway (hsa04330), and chronic
244 myeloid leukemia (hsa05220). along with pathways in cancer and small cell lung cancer. The
245 detailed module enrichment result is shown in Supplementary Table 6.



247 Figure 4: Summary of genes identified from multi-omics analysis and their potential role in each of the hallmarks of
248 endometriosis.

249 Discussion

250 We report the largest multi-population GWAS for endometriosis to date incorporating
251 nearly a million participants from 14 diverse biobanks across the world and increasing the total
252 number of GWAS loci. Although multiple significant loci obtained from our study have been
253 previously implicated in endometriosis pathophysiology, we have identified seven previously
254 unreported GWAS loci and two previously unreported TWAS genes associated with
255 endometriosis, which provides important insights into the underlying genetic architecture of
256 endometriosis across population. We have summarized the major associations based on their
257 involvement in specific biological functions (increased sex steroid hormones, immune
258 regulation, inflammation, cell morphogenesis and vascular development and remodeling) in
259 Figure 4, these could also be defined as five hallmarks of endometriosis.

260 Our ancestry stratified meta-analyses revealed a consistent observed SNP heritability of
261 10-12% for endometriosis for three studied genetic ancestry populations (EUR, EAS, and AFR),
262 which is higher than previously observed SNP heritability of 7% based solely on European
263 populations. The higher and more consistent heritability we observed can be attributed to the
264 unprecedented scale and diversity of our study cohort. The previous GWASs have not included
265 any African-ancestry or Admixed-American-ancestry (AMR) populations, which were essential
266 in the computation of 14 / 38 (37%) credible sets in our fine-mapping analysis. We detected
267 one African-only GWAS locus, *POLR2M*, and one AMR-only MAGMA gene, *CEBPE*. By

268 incorporating biobanks from various regions and ancestry backgrounds worldwide, we were
269 able to capture a more comprehensive genetic landscape of endometriosis.

270 Given that diagnosis codes from the EHR can be unreliable for accurately phenotyping
271 endometriosis, we employed narrow phenotyping algorithms which incorporated procedure
272 codes (surgical and imaging). Despite the diminished sample sizes, there were still genome-
273 wide significant loci: one for PCN.v1, two for SCN.v1, and two for SCN.v2. Both GWAS loci for
274 SCN.v2 (*KCNF1* and *12q24.32*) were successfully fine-mapped, with five and two putative causal
275 variants in their credible sets, respectively. The EAS-only PCN.v1 meta-analysis yielded a
276 significantly enriched gene, *HAVCR2*, an immune receptor gene near the *5q33.3* GWAS locus,
277 which was not present in the other meta-analyses. Leveraging multi-modal EHR data for more
278 precise phenotyping significantly enhanced our ability to refine and validate genetic
279 associations and uncover deeper biological insights.

280 Our meta-GWAS and PWAS analyses underscore the potential role of *RSPO3* in
281 endometriosis pathophysiology. *RSPO3*, previously known to modulate risk of endometriosis,
282 interacts with *WNT4* via Frizzled (*FZD*) receptors, influencing the WNT/Ca²⁺ and WNT/ β -catenin
283 pathways^{27,28}. *WNT4* interacts with *ESR1* (Estrogen Receptor Alpha), key regulator of
284 endometrial cell proliferation and survival throughout the menstrual cycle²⁹. Additionally,
285 scDRS analyses identified *ESR1*, *WNT4*, *SYNE1*, *GREB1*, *IGF1*, and *FSHB* as relevant in
286 endometrial perivascular cells (ePV) from donors in the secretory phase, while *RMND1*
287 (Required for Meiotic Nuclear Division 1 homolog), *ARMT1*, and *CCDC170* were linked to
288 secretory phase ciliated cells. Collectively, these genes likely promote increased sex steroid
289 hormone production and signaling. This hormonal milieu may, in turn, fuel inflammatory

290 responses and dysregulate immune function, potentially driving the progression of
291 endometriosis^{6,30,31}.

292 Our meta-GWAS and TWAS analyses identified *VEZT* (Vezatin) and *ARL14EP* as
293 significant. *VEZT* exhibits menstrual cycle-dependent expression in endometrial glands during
294 the secretory phase and is also relevant in venous cells of individuals on exogenous
295 hormones³². Together with *FGD6*, *VEZT* plays a crucial role in cytoskeletal remodeling.
296 Dysregulation of this process can accelerate cell proliferation, migration, and invasion into the
297 endometrium, promoting the development of ectopic lesions. This dysregulation may also lead
298 to uncontrolled epithelial-mesenchymal transition (EMT), potentially driving endometriosis
299 progression^{32,33}. *ARL14EP* has previously been linked to depression which is a known
300 endometriosis comorbidity³⁴. It was also prominent in ciliated cells from the secretory phase in
301 scDRS analysis. *ARL14EP* is involved in MHCII movement via the TGF- β pathway, suggesting a
302 role in immune modulation, a hallmark of endometriosis^{35,36}. Last, we also identified *VEGFR2*
303 (*KDR*), significant in arterial cells from the secretory phase, and *CDKN2A*, both known to
304 regulate angiogenesis and endothelial cell adhesion^{37,38}. *CDC42*, another significant hit, plays a
305 role in vascular remodeling along with *VEGFR2*³⁹⁻⁴¹. Together, these findings highlight pathways
306 in vascular and immune modulation, guiding future functional studies on endometriosis.

307 Despite the large sample size, heritability observed with GWAS (10-12%) still fails to
308 measure up to the broad sense heritability estimation from a twin study of 47%⁴². Rare
309 variants, structural variants, nonlinear effects, or gene-environment interactions might
310 contribute to endometriosis risk but remain undetected in our analyses. As we leveraged the
311 GWAS results to study other levels of the central dogma, one limitation was that we lacked

312 individual-level transcriptomic/proteomic data. The TWAS and PWAS performance relied on
313 previously-trained *cis*-eQTL expression models, limiting the power, since the models do not
314 capture all the gene expression variability and complex genetic architecture potentially relevant
315 to our phenotype of interest⁴³. Mergeomics assumes that overlapping signals between GWAS,
316 TWAS, and PWAS are biologically relevant. The tool primarily considers only the association p-
317 value, but not the directionality of association, which may limit the validity of detected
318 biological signals. Additionally, Mergeomics may not fully capture complex interactions
319 between genes or the functional effects of non-coding variants. While this tool does not allow
320 us to infer causality, it does generate testable biological hypotheses for further functional
321 assays.

322 In addition to replicating findings from previous studies, we uncovered new insights that
323 advanced our understanding of the genetic underpinnings of endometriosis. Our integrative
324 multi-omics approach, combining genomic data with transcriptomic, proteomic, and single-cell
325 analyses, has provided unprecedented insights into the molecular mechanisms driving this
326 chronic condition. These findings lay a robust foundation for future functional studies to
327 elucidate the precise roles of identified genes and pathways in endometriosis pathogenesis.
328 Moreover, our results have important clinical implications, potentially informing the
329 development of more accurate diagnostic tools, personalized risk prediction models, and
330 targeted therapeutic interventions. As we move forward, this work emphasizes the critical
331 importance of large-scale, diverse genetic studies in unraveling the complexities of
332 multifactorial diseases like endometriosis, paving the way for improved patient outcomes and a
333 deeper understanding of women's health issues globally.

334 **Methods**

335 **Phenotyping**

336 For the EHR-linked biobanks, we used structured data to define the phenotypes. Cases for wide
337 endometriosis (W) were any women with a history of ICD-9, ICD-10, or SNOMED codes for
338 endometriosis. For the wide phenotype excluding adenomyosis (Wex), women with a history of
339 ICD-9, ICD-10, or SNOMED codes for uterine endometriosis were excluded from both cases and
340 controls. Our two narrow case definitions were procedure-confirmed and surgically-confirmed
341 (PCN and SCN). These narrow phenotypes were designed to capture confirmed cases and
342 controls of endometriosis based on procedure history including hysterectomies, laparoscopies
343 and ultrasounds. The list of procedure codes (CPT-4 or OPCS) for PCN included all the surgery
344 codes in SCN but added non-obstetric ultrasound codes to account for potential imaging
345 diagnoses. Each of the two narrow phenotypes was tested in two versions: cases versus all
346 controls (PCN.v1 and SCN.v1) and cases versus confirmed controls (PCN.v2 and SCN.v2) where
347 confirmed controls were those who had history of the corresponding procedure codes for each
348 phenotype with no history of endometriosis diagnosis. For additional details on the
349 phenotyping algorithms, see Supplemental Appendix 1.

350 **Genotyping by Biobank**

351 Most contributing biobanks acquired several hundred thousand variants. After those data are
352 collected, then the rest of the genomic variants can be imputed probabilistically based on a
353 reference panel such as TOPMED. Some biobanks used short read whole genome sequencing
354 (WGS) to gather their genomic data. The sequences from the short reads are aligned and

355 compared to the reference to produce variant calls. References and platform information for
356 each biobank's genotyping method and QC can be found in Supplemental Appendix 2.

357 **Genetic Association Testing**

358 Each contributing biobank performed ancestry-stratified association testing with up to six
359 phenotypes (W, Wex, PCN.v1, PCN.v2, SCN.v1, and SCN.v2), depending on whether they had at
360 least 50 cases for that phenotype and ancestry combination. Genetically-informed ancestry
361 (GIA) is defined based on genetic distance from subpopulations of a reference group such as
362 the 1000 Genomes Project dataset⁴⁴ (1KG). Genetic distance is measured using a dimensionality
363 reduction technique such as principal component analysis (PCA). Ancestry is then assigned
364 using a classifier such as a mixture model or k-nearest neighbors. For references and methods
365 used for assigning GIA within each biobank, see Supplemental Appendix 3.

366 Contributing biobanks used linear mixed models to estimate the effect of each variant
367 on the six phenotypes. Tools implemented for these tests include SAIGE⁴⁵ and Regenie⁴⁶.
368 Association tests were adjusted for principal components, age at EHR data collection, and any
369 biobank-specific batch variables (for example, collection site within eMERGE). For estimation of
370 the null models (SAIGE or Regenie step 1), variants were required to have a call rate of at least
371 95%, a minor allele frequency of 0.01, and a Hardy-Weinberg p-value of at least 1×10^{-6} . For
372 association testing (SAIGE or Regenie step 2), variants were required to have a minor allele
373 count of at least 20, and an imputation quality of at least 0.6. Individuals were included if their
374 overall genotyping rate was at least 95%. A summary of each biobank's exact covariates and QC
375 procedures is in Supplemental Appendix 4.

376 After biobank analyses were completed and collected, summary statistics were cleaned
377 and lifted into genome build hg38 as necessary. Then, inverse variance-weighted, fixed-effect
378 meta-analyses were performed using GWAMA⁴⁷. GWAMA adjusts each study based on its
379 overall genomic inflation factor. Prior to meta-analysis, input summary statistics were restricted
380 to variants with a minor allele frequency of at least 0.005 to ensure stability in the estimates.
381 We started by applying the clumping function of Plink 1.9⁴⁸ with the lead SNP p-value threshold
382 set to 5×10^{-8} , the secondary SNP threshold set to 1×10^{-3} , minimum R^2 of 0.1, and a window of
383 1000kb. 1KG was used as a linkage disequilibrium (LD) reference since the meta-analyses were
384 multi-ancestry. After the variant clumps were identified, any clumps that were physically
385 overlapping with one another were merged into loci. Then, we tested if any loci were in LD with
386 ($R^2 > 0.25$) or proximal to tag SNPs of the 39 autosomal lead SNPs from the 2023 GWAS⁴⁹ to
387 determine whether our hits were known or previously unreported¹⁰.

388 **Estimation of Observed SNP Heritability**

389 We estimated heritability with the LD-Score Regression tool, LDSC⁵⁰, for four ancestry-
390 stratified meta-analyses and the multi-ancestry meta-analysis. LD scores were computed from
391 the full 1KG for the multi-ancestry summary statistics, and from the respective super-
392 population subgroups from 1KG for each ancestry-stratified meta-analysis.

393 **Variant-Set Enrichment for Identifying Enriched Gene Regions**

394 MAGMA⁵¹ was used to assess gene regions within the GWAS results for enrichment.
395 MAGMA uses a model based on multiple regression to test the association of a phenotype with
396 groups of variants. Testing groups of variants increases statistical power over the single-variant

397 GWAS tests performed⁵¹. We utilized gene region definitions from NCBI for human genome
398 build 38, testing about 18,000 genes for each GWAS.

399 **Statistical Fine-Mapping for Identification of Putative Causal Variants**

400 MESuSiE⁵² was used to identify causal variants in each significant GWAS locus. We
401 extracted the summary statistics from each locus's region in addition to computing LD matrices
402 for that region in all ancestry groups comprising the overall study. For single-ancestry meta-
403 analyses, only one LD matrix was needed, but the loci from the multi-ancestry meta-analyses
404 were fine-mapped using LD matrices from AFR, AMR, EAS, and EUR. MESuSiE analyzes whether
405 causal variants are shared between ancestry groups by computing a posterior probability of
406 causality (PIP) for each ancestry alone and for each combination of two or more ancestries.
407 SNPs with any PIP value greater than 0.5 are part of the credible set for that locus.

408 **Tissue-Specific Transcriptome-Wide Association Study**

409 We used GWAS summary statistics from our multi-population W meta-analysis to
410 estimate the association between the variants on expression of genes and the complex trait,
411 endometriosis. We used precomputed eQTL weights from the PredictDB data repository
412 (<http://predictdb.org/>) which represented *cis*-level associations. The database files comprise of
413 a list of genetic variants (*cis*-SNPs) used to predict gene expression, located within 1 Mb of a
414 gene, eQTL weights, and covariance information. Those models along with the GWAS summary
415 statistics were input into the summary-based PrediXcan (S-PrediXcan) pipeline for the
416 transcriptome-wide association study (TWAS), scanning for genes whose expression levels were
417 associated with endometriosis⁵³. We used Bonferroni $P < 0.05$ (corrected for 9,642 tests) to
418 identify statistically significant TWAS genes.

419 **Proteome-Wide Association Study**

420 We performed a proteome-wide association study (PWAS) to investigate the association
421 between genetically predicted protein levels and endometriosis. We used summary-level GWAS
422 data from the multi-ancestry W meta-analysis, and pQTL models developed by *Schubert et al*⁵⁴.
423 The models were derived from SOMAscan assay of plasma proteins measured in multi-ethnic
424 Trans-omics for Precision Medicine (TOPMed) Multi-omics pilot study, capturing 1mb cis-
425 regulatory window. We used baseline models only, essentially those models were trained under
426 standard conditions without any additional adjustments for other covariates or interaction
427 terms, typically a reference model for general prediction of gene expression based solely on
428 genetic variation. Only models with a predictive correlation (ρ) of at least 0.1 and a z-score p-
429 value threshold of 0.05, meaning that the association between the SNPs and gene expression is
430 statistically significant, were included. The PWAS was thereby performed on 309 most robust,
431 and reliable models for the analysis. We employed the S-PrediXcan pipeline to perform the
432 PWAS. We used Bonferroni-correct P value threshold ($P < 0.05 / 309$) for identifying significant
433 PWAS genes.

434 **Integration with Single-Cell Data**

435 Single cell data are rich resources for understanding the biology of diseases. A recently-
436 published endometrial single cell atlas includes gene expression data for cells, nuclei, immune
437 cells, and immune nuclei, covering over 40 different cell types, three menstrual phases, and
438 four different endometrial pathologies⁵⁵. We leveraged these data to compute single-cell
439 disease-relevance scores (scDRSs) based on the associated genes from the GWAS, as computed
440 by MAGMA. Disease risk scores were computed and normalized using the scDRS software⁵⁶. We

441 removed any cell types labeled as “hormones,” as the authors did in the atlas release paper
442 when they performed fGWAS.

443 For each cell type and menstrual phase, we compared the scDRSs of cells from donors
444 with and without endometriosis. We performed one-sided t-tests to compare the distributions,
445 hypothesizing that the scDRSs of cells from endometriosis cases should be higher than that of
446 cells from endometriosis controls. We also computed the area under the receiver-operating
447 curve (AUROC) to see how well the scDRS distinguished between endometriosis case and
448 control donors. From there, we prioritized cell type – menstrual phase combinations with
449 significant t-tests and AUROC > 0.6 for further examination. We compared the expression of the
450 top MAGMA genes between case and control donors using t-tests to identify which genes were
451 driving the performance of the scDRS.

452 **Merge-Omics**

453 Using the GWAS, TWAS, and PWAS results, we conducted a marker set enrichment analysis
454 (MSEA) with Mergeomics²⁴. MSEA identifies key marker sets (genes or proteins) significantly
455 enriched for associations across multi-omics data. The markers were mapped to Kyoto
456 Encyclopedia of Genes and Genomes (KEGG) pathways using gene annotations. We used GWAS,
457 TWAS and PWAS markers (rsIDs for GWAS and gene names for TWAS and PWAS), along with
458 their corresponding $-\log_{10}$ transformed p-values as input for the tool. We enriched for KEGG
459 pathways with FDR < 0.05.

460 **Acknowledgments**

461 Research reported in this publication was supported by the Eunice Kennedy Shriver National
462 Institute of Child Health and Human Development of the National Institutes of Health under
463 award number R01HD110567.

464 We acknowledge the Penn Medicine BioBank (PMBB) for providing data and thank the patient-
465 participants of Penn Medicine who consented to participate in this research program. We
466 would also like to thank the Penn Medicine BioBank team and Regeneron Genetics Center for
467 providing genetic variant data for analysis. The PMBB is approved under IRB protocol# 813913
468 and supported by Perelman School of Medicine at University of Pennsylvania, a gift from the
469 Smilow family, and the National Center for Advancing Translational Sciences of the National
470 Institutes of Health under CTSA award number UL1TR001878.

471 This phase of the eMERGE Network was initiated and funded by the NHGRI through the
472 following grants: U01HG008657 (Group Health Cooperative/University of Washington);
473 U01HG008685 (Brigham and Women's Hospital); U01HG008672 (Vanderbilt University Medical
474 Center); U01HG008666 (Cincinnati Children's Hospital Medical Center); U01HG006379 (Mayo
475 Clinic); U01HG008679 (Geisinger Clinic); U01HG008680 (Columbia University Health Sciences);
476 U01HG008684 (Children's Hospital of Philadelphia); U01HG008673 (Northwestern University);
477 U01HG008701 (Vanderbilt University Medical Center serving as the Coordinating Center);
478 U01HG008676 (Partners Healthcare/Broad Institute); and U01HG008664 (Baylor College of
479 Medicine).

480 We gratefully acknowledge All of Us participants for their contributions, without whom this
481 research would not have been possible. We also thank the National Institutes of Health's All of
482 Us Research Program for making available the participant data examined in this study.

483 This research has been conducted using the Taiwan Biobank Resource. We thank all the
484 participants and investigators of the Taiwan Biobank. We thank the National Center for
485 Genome Medicine, Academia Sinica, Taiwan, for the technical support in the genotyping.
486 We thank National Core Facility for Biopharmaceuticals (NCFB, 112-2740-B-492-001) and
487 National Center for High-performance Computing (NCHC) of National Applied Research
488 Laboratories (NARLabs) of Taiwan for providing computational resources and storage
489 resources. This study was supported by the National Health Research Institutes (NP-109, 110,
490 111, 112, 113-PP-09), Ministry of Science and Technology (MOST 109-2314-B-400-017, 110-
491 2314-B-400-028-MY3), and National Science and Technology Council (NSCT 113-2628-B-400-
492 002), Taiwan.

493 The Trøndelag Health Study (The HUNT Study) is a collaboration between HUNT Research
494 Centre (Faculty of Medicine and Health Sciences, NTNU, Norwegian University of Science and
495 Technology), Trøndelag County Council, Central Norway Regional Health Authority, and the
496 Norwegian Institute of Public Health. The genotyping in HUNT was financed by the National
497 Institutes of Health; University of Michigan; the Research Council of Norway; the Liaison
498 Committee for Education, Research and Innovation in Central Norway; and the Joint Research
499 Committee between St Olavs hospital and the Faculty of Medicine and Health Sciences, NTNU.
500 The genetic investigations of the HUNT Study are a collaboration between researchers from the
501 HUNT Center for Molecular and Clinical Epidemiology (formerly known as the K.G. Jebsen

502 Center for Genetic Epidemiology as of August 1st 2023), NTNU, and the University of Michigan
503 Medical School and the University of Michigan School of Public Health. We thank HUNT
504 participants for donating their time, samples, and information to help others; clinicians and
505 other employees at Nord-Trøndelag Hospital Trust for their support and for contributing to data
506 collection.

507 **References**

- 508 1. Christ, J. P. *et al.* Incidence, prevalence, and trends in endometriosis diagnosis: a United
509 States population-based study from 2006 to 2015. *American Journal of Obstetrics and*
510 *Gynecology* **225**, 500.e1-500.e9 (2021).
- 511 2. Agarwal, S. K. *et al.* Clinical diagnosis of endometriosis: a call to action. *American Journal of*
512 *Obstetrics and Gynecology* **220**, 354.e1-354.e12 (2019).
- 513 3. Fauconnier, A. & Chapron, C. Endometriosis and pelvic pain: epidemiological evidence of
514 the relationship and implications. *Human Reproduction Update* **11**, 595–606 (2005).
- 515 4. Coccia, M. E., Nardone, L. & Rizzello, F. Endometriosis and Infertility: A Long-Life Approach
516 to Preserve Reproductive Integrity. *International Journal of Environmental Research and*
517 *Public Health* **19**, 6162 (2022).
- 518 5. Fatumo, S. *et al.* A roadmap to increase diversity in genomic studies. *Nat Med* **28**, 243–250
519 (2022).
- 520 6. Sapkota, Y. *et al.* Meta-analysis identifies five novel loci associated with endometriosis
521 highlighting key genes involved in hormone metabolism. *Nat Commun* **8**, 15539 (2017).

- 522 7. Rahmioglu, N. *et al.* The genetic basis of endometriosis and comorbidity with other pain and
523 inflammatory conditions. *Nat Genet* **55**, 423–436 (2023).
- 524 8. Verma, A. *et al.* The Penn Medicine BioBank: Towards a Genomics-Enabled Learning
525 Healthcare System to Accelerate Precision Medicine in a Diverse Population. *Journal of*
526 *Personalized Medicine* **12**, 1974 (2022).
- 527 9. Genomic data in the All of Us Research Program. *Nature* **627**, 340–346 (2024).
- 528 10. Verma, A. *et al.* Diversity and Scale: Genetic Architecture of 2,068 Traits in the VA Million
529 Veteran Program. 2023.06.28.23291975 Preprint at
530 <https://doi.org/10.1101/2023.06.28.23291975> (2023).
- 531 11. Zhou, W. *et al.* Global Biobank Meta-analysis Initiative: Powering genetic discovery across
532 human disease. *Cell Genomics* **2**, 100192 (2022).
- 533 12. Nagai, A. *et al.* Overview of the BioBank Japan Project: Study design and profile. *Journal of*
534 *Epidemiology* **27**, S2–S8 (2017).
- 535 13. Pulley, J., Clayton, E., Bernard, G. R., Roden, D. M. & Masys, D. R. Principles of human
536 subjects protections applied in an opt-out, de-identified biobank. *Clin Transl Sci* **3**, 42–48
537 (2010).
- 538 14. Roden, D. *et al.* Development of a Large-Scale De-Identified DNA Biobank to Enable
539 Personalized Medicine. *Clinical Pharmacology & Therapeutics* **84**, 362–369 (2008).
- 540 15. Wiley, L. K. *et al.* Building a vertically integrated genomic learning health system: The
541 biobank at the Colorado Center for Personalized Medicine. *The American Journal of Human*
542 *Genetics* **111**, 11–23 (2024).

- 543 16. Gottesman, O. *et al.* The Electronic Medical Records and Genomics (eMERGE) Network:
544 past, present, and future. *Genet Med* **15**, 761–771 (2013).
- 545 17. David, S. P. *et al.* Personalized medicine in a community health system: the NorthShore
546 experience. *Front. Genet.* **14**, (2023).
- 547 18. Brumpton, B. M. *et al.* The HUNT study: A population-based cohort for genetic research.
548 *Cell Genomics* **2**, (2022).
- 549 19. Rovite, V. *et al.* Genome Database of the Latvian Population (LGDB): Design, Goals, and
550 Primary Results. *Journal of Epidemiology* **28**, 353–360 (2018).
- 551 20. Boutin, N. T. *et al.* The Evolution of a Large Biobank at Mass General Brigham. *Journal of*
552 *Personalized Medicine* **12**, 1323 (2022).
- 553 21. Fan, C.-T., Lin, J.-C. & Lee, C.-H. Taiwan Biobank: A Project Aiming to Aid Taiwan’s Transition
554 into a Biomedical Island. *Pharmacogenomics* **9**, 235–246 (2008).
- 555 22. Bycroft, C. *et al.* The UK Biobank resource with deep phenotyping and genomic data. *Nature*
556 **562**, 203–209 (2018).
- 557 23. Katon, J. G., Plowden, T. C. & Marsh, E. E. Racial disparities in uterine fibroids and
558 endometriosis: a systematic review and application of social, structural, and political
559 context. *Fertility and Sterility* **119**, 355–363 (2023).
- 560 24. Ding, J. *et al.* Mergeomics 2.0: a web server for multi-omics data integration to elucidate
561 disease networks and predict therapeutics. *Nucleic Acids Research* **49**, W375–W387 (2021).
- 562 25. Kurki, M. I. *et al.* FinnGen provides genetic insights from a well-phenotyped isolated
563 population. *Nature* **613**, 508–518 (2023).

- 564 26. Kanehisa, M. & Goto, S. KEGG: Kyoto Encyclopedia of Genes and Genomes. *Nucleic Acids*
565 *Research* **28**, 27–30 (2000).
- 566 27. Tao, T., Mo, X. & Zhao, L. Identifying novel potential drug targets for endometriosis via
567 plasma proteome screening. *Front. Endocrinol.* **15**, (2024).
- 568 28. Scholz, B. *et al.* Endothelial RSPO3 Controls Vascular Stability and Pruning through Non-
569 canonical WNT/Ca²⁺/NFAT Signaling. *Developmental Cell* **36**, 79–93 (2016).
- 570 29. Gallagher, C. S. *et al.* Genome-wide association and epidemiological analyses reveal
571 common genetic origins between uterine leiomyomata and endometriosis. *Nat Commun*
572 **10**, 4857 (2019).
- 573 30. Marla, S. *et al.* Genetic risk factors for endometriosis near estrogen receptor 1 and
574 coexpression of genes in this region in endometrium. *Molecular Human Reproduction* **27**,
575 gaaa082 (2021).
- 576 31. García-Gómez, E. *et al.* Regulation of Inflammation Pathways and Inflammasome by Sex
577 Steroid Hormones in Endometriosis. *Front. Endocrinol.* **10**, (2020).
- 578 32. Holdsworth-Carson, S. J. *et al.* Endometrial vezatin and its association with endometriosis
579 risk. *Human Reproduction* **31**, 999–1013 (2016).
- 580 33. Szymański, M. *et al.* Role of Cyclins and Cytoskeletal Proteins in Endometriosis: Insights into
581 Pathophysiology. *Cancers* **16**, 836 (2024).
- 582 34. Adewuyi, E. O. *et al.* Genetic analysis of endometriosis and depression identifies shared loci
583 and implicates causal links with gastric mucosa abnormality. *Hum Genet* **140**, 529–552
584 (2021).

- 585 35. Paul, P. *et al.* A Genome-wide Multidimensional RNAi Screen Reveals Pathways Controlling
586 MHC Class II Antigen Presentation. *Cell* **145**, 268–283 (2011).
- 587 36. Hogg, C. *et al.* Macrophages inhibit and enhance endometriosis depending on their origin.
588 *Proceedings of the National Academy of Sciences* **118**, e2013776118 (2021).
- 589 37. Jin, Y. *et al.* Deletion of Cdc42 Enhances ADAM17-Mediated Vascular Endothelial Growth
590 Factor Receptor 2 Shedding and Impairs Vascular Endothelial Cell Survival and
591 Vasculogenesis. *Molecular and Cellular Biology* **33**, 4181–4197 (2013).
- 592 38. Barry, D. M. *et al.* Cdc42 is required for cytoskeletal support of endothelial cell adhesion
593 during blood vessel formation in mice. *Development* **142**, 3058–3070 (2015).
- 594 39. Sugino, N., Kashida, S., Karube-Harada, A., Takiguchi, S. & Kato, H. Expression of vascular
595 endothelial growth factor (VEGF) and its receptors in human endometrium throughout the
596 menstrual cycle and in early pregnancy. (2002) doi:10.1530/rep.0.1230379.
- 597 40. Cerione, R. A. Cdc42: new roads to travel. *Trends in Cell Biology* **14**, 127–132 (2004).
- 598 41. Slack, M. A. & Gordon, S. M. Protease Activity in Vascular Disease. *Arterioscler Thromb Vasc*
599 *Biol* **39**, e210–e218 (2019).
- 600 42. Saha, R. *et al.* Heritability of endometriosis. *Fertility and Sterility* **104**, 947–952 (2015).
- 601 43. Mai, J., Lu, M., Gao, Q., Zeng, J. & Xiao, J. Transcriptome-wide association studies: recent
602 advances in methods, applications and available databases. *Commun Biol* **6**, 1–10 (2023).
- 603 44. An integrated map of genetic variation from 1,092 human genomes. *Nature* **491**, 56–65
604 (2012).
- 605 45. Zhou, W. *et al.* Efficiently controlling for case-control imbalance and sample relatedness in
606 large-scale genetic association studies. *Nat Genet* **50**, 1335–1341 (2018).

- 607 46. Mbatchou, J. *et al.* Computationally efficient whole-genome regression for quantitative and
608 binary traits. *Nat Genet* **53**, 1097–1103 (2021).
- 609 47. Mägi, R. & Morris, A. P. GWAMA: software for genome-wide association meta-analysis.
610 *BMC Bioinformatics* **11**, 288 (2010).
- 611 48. Purcell, S. *et al.* PLINK: A Tool Set for Whole-Genome Association and Population-Based
612 Linkage Analyses. *Am J Hum Genet* **81**, 559–575 (2007).
- 613 49. Rahmioglu, N. *et al.* The genetic basis of endometriosis and comorbidity with other pain and
614 inflammatory conditions. *Nat Genet* **55**, 423–436 (2023).
- 615 50. LD Score regression distinguishes confounding from polygenicity in genome-wide
616 association studies | Nature Genetics. <https://www.nature.com/articles/ng.3211>.
- 617 51. Leeuw, C. A. de, Mooij, J. M., Heskes, T. & Posthuma, D. MAGMA: Generalized Gene-Set
618 Analysis of GWAS Data. *PLOS Computational Biology* **11**, e1004219 (2015).
- 619 52. Gao, B. & Zhou, X. MESuSiE enables scalable and powerful multi-ancestry fine-mapping of
620 causal variants in genome-wide association studies. *Nat Genet* **56**, 170–179 (2024).
- 621 53. Gamazon, E. R. *et al.* A gene-based association method for mapping traits using reference
622 transcriptome data. *Nat Genet* **47**, 1091–1098 (2015).
- 623 54. Schubert, R. *et al.* Protein prediction for trait mapping in diverse populations. *PLOS ONE* **17**,
624 e0264341 (2022).
- 625 55. Marečková, M. *et al.* An integrated single-cell reference atlas of the human endometrium.
626 *Nat Genet* **56**, 1925–1937 (2024).
- 627 56. Zhang, M. J. *et al.* Polygenic enrichment distinguishes disease associations of individual cells
628 in single-cell RNA-seq data. *Nat Genet* **54**, 1572–1580 (2022).

